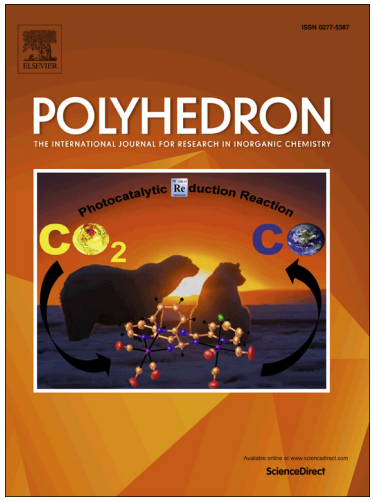

Dinuclear niobium(III), tantalum(III) and tantalum(IV) complexes with thioether and selenoether ligands

Sophie L. Benjamin, Yao-Pang Chang, Michelle Huggon, William Levason, Gillian Reid

PII: S0277-5387(15)00417-9
DOI: http://dx.doi.org/10.1016/j.poly.2015.07.062
Reference: POLY 11448

To appear in: *Polyhedron*

Received Date: 27 June 2015
Accepted Date: 27 July 2015

Please cite this article as: S.L. Benjamin, Y-P. Chang, M. Huggon, W. Levason, G. Reid, Dinuclear niobium(III), tantalum(III) and tantalum(IV) complexes with thioether and selenoether ligands, *Polyhedron* (2015), doi: http://dx.doi.org/10.1016/j.poly.2015.07.062

Dinuclear niobium(III), tantalum(III) and tantalum(IV) complexes with thioether and selenoether ligands

Sophie L. Benjamin[a], Yao-Pang Chang[b], Michelle Huggon[b], William Levason[b] and Gillian Reid[b]*

a School of Science and Technology, Nottingham Trent University, Nottingham NG11 8NS, UK

b School of Chemistry, University of Southampton, Highfield, Southampton SO17 1BJ, UK.

Abstract

Magnesium reduction of MCl_5 (M = Nb or Ta) in the presence of R_2S (R = Me or ^{n}Bu) affords the complexes $[M_2Cl_4(R_2S)_2(\mu\text{-}Cl)_2(\mu\text{-}R_2S)]$. The X-ray structures of those complexes where M = Nb or Ta, R = ^{n}Bu$_2$S, and of a new polymorph of $[Ta_2Cl_4(Me_2S)_2(\mu\text{-}Cl)_2(\mu\text{-}Me_2S)]$, show that they have confacial bi-octahedral structures with M=M double bonds. The reactions of $[Nb_2Cl_4(R_2S)_2(\mu\text{-}Cl)_2(\mu\text{-}R_2S)]$ with $MeSCH_2CH_2SMe$, $MeSeCH_2CH_2SeMe$ or $MeSeCH_2CH_2CH_2SeMe$ produce the edge-linked dimers $[Nb_2Cl_4(MeSCH_2CH_2SMe)_2(\mu\text{-}Cl)_2]$ and $[Nb_2Cl_4\{MeSe(CH_2)_nSeMe\}_2(\mu\text{-}Cl)_2]$, all with M=M double bonds (M_2^{6+}). The tantalum diselenoether complex, $[Ta_2Cl_4(MeSeCH_2CH_2SeMe)_2(\mu\text{-}Cl)_2]$, is similar. Two "dimer of dimers", $[\{Nb_2Cl_4(\mu\text{-}Cl)_2(\mu\text{-}Me_2S)\}_2(\mu\text{-}MeSeCH_2CH_2CH_2SeMe)_2]$ and $[\{Ta_2Cl_4(\mu\text{-}Cl)_2(\mu\text{-}Me_2S)\}_2(\mu\text{-}^nBuSeCH_2CH_2CH_2Se^nBu)_2]$, containing confacial bi-octahedra linked by diselenoether bridges, were obtained as minor by-products and were identified *via* their X-ray crystal structures. The xylyl-linked diselenoether, *o*-$C_6H_4(CH_2SeMe)_2$, gave a complex mixture of products, including $[Ta_2Cl_4\{o\text{-}C_6H_4(CH_2SeMe)_2\}_2(\mu\text{-}Se)_2]$. The complexes were characterised by microanalysis, IR and UV-visible spectroscopy. X-ray crystal structures are reported for $[Nb_2Cl_6(^nBu_2S)_3]$, $[Ta_2Cl_6(^nBu_2S)_3]$, $[Ta_2Cl_8(Me_2S)_2]$, $[Ta_2Cl_6(Me_2S)_3]$, $[Ta_2Cl_4\{o\text{-}C_6H_4(CH_2SeMe)_2\}_2(Se)_2]$, $[\{Ta_2Cl_6(Me_2S)(^nBuSeCH_2CH_2CH_2Se^nBu)\}_2]$ and $[Ta_2Cl_4(Me_2S)_4(S)_2]$.

Keywords: niobium, tantalum, thioether, selenoether, X-ray structure

1. Introduction

Niobium and tantalum exhibit a rich coordination chemistry spanning eight formal oxidation states (–III to +V) [1]. In addition to the inherent interest, understanding this complex coordination

chemistry is necessary for the development of new functional materials containing these elements, which have applications in electronics, magnetism and energy storage. Key examples are early transition metal dichalcogenides (ME_2 E = S, Se or Te; M = Nb or Ta), which have layered structures and their properties may be tuned by choice of M and E [2-7]. Thin films of these substances are of particular interest since 2D layers maximise the anisotropy of the material properties. Production of thin films by exfoliation of bulk samples [8] or chemical vapour deposition (CVD) from either single or dual source precursors [9-12], are current methods of choice. Single source CVD reagents minimise the quantity of reagent needed and potentially offer better control over the composition and film thickness, but reagents suitable for deposition of the heavier analogues (E = Se or Te) are rare [11,12]. We recently reported that thin films of NbE_2 (E = S or Se) can be deposited onto silica substrates using low pressure CVD (LPCVD) from $[NbCl_5(E^nBu_2)]$, although the analogous tantalum complexes were unsuitable [13]. We therefore initiated studies of a wider range of Nb and Ta complexes as potential CVD precursors. LPCVD requires the precursors to vapourise under reduced pressure, but the alternative technique of aerosol assisted CVD (AACVD) provides an aerosol of the reagent from a suitable solvent and may be useful for complexes of insufficient volatility for LPCVD. Here we report on the study of some dinuclear complexes of Nb and Ta in oxidation states III or IV and their evaluation as possible CVD precursors.

Complexes of type $[M_2Cl_6(L)_3]$ (M = Nb or Ta, L = Me_2S or tetrahydrothiophene) are prepared by reduction of the corresponding MCl_5 with Na/Hg or Mg in the presence of excess of the S-donor ligand [1,14-16]. The structures contain confacial bioctahedra $[M_2L_2Cl_4(\mu\text{-}Cl)_2(\mu\text{-}L)]$ with M=M double bonds [15,17]. Reactions of the dimers with bidentate ligands, e.g. 2,5-dithiahexane or 3,6-dithiaoctane, were reported to give $[M_2Cl_4(RSCH_2CH_2SR)_2(\mu\text{-}Cl)_2]$, identified as $M=M^{6+}$ edge-sharing bioctahedra [18,19]. Oxidative addition of Ph_2S_2 to $[Ta_2Cl_6(Me_2S)_3]$ gave the $Ta=Ta^{6+}$ dimer, $[Ta_2Cl_4(Me_2S)_2(\mu\text{-}SPh)_2]$ [20]. However, a re-examination of the $[Ta_2Cl_4(EtSCH_2CH_2SEt)_2(\mu\text{-}Cl)_2]$ complex and of $[M_2Cl_6(Me_2S)_4]$ showed that these were in fact sulfide-bridged, rather than chloride-bridged and should be formulated $[Ta_2Cl_4(EtSCH_2CH_2SEt)_2(\mu\text{-}S)_2]$ and $[M_2Cl_4(Me_2S)_4(\mu\text{-}S)_2]$, containing single M–M bonds, and hence M(IV) rather than M(III) centres [18,21]. The niobium complex, $[Nb_2Cl_4(EtSCH_2CH_2SEt)_2(\mu\text{-}Cl)_2]$, is correctly formulated as Nb=Nb. These studies reveal the complicated synthetic chemistry and structural relationships in these systems. The isoelectronic Cl^- and S^{2-} are extremely difficult to distinguish by X-ray crystallography, and the best current indicator is the metal-metal bond length, which should distinguish M=M from M–M. It is clear that small changes

to the reaction conditions can lead to different products (or mixtures of products), and, as pointed out by Cotton [21], other reported compounds of these types may be incorrectly formulated.

2. Experimental

Infrared spectra were recorded as Nujol mulls or thin films between CsI plates using a Perkin Elmer Spectrum 100 over the range 4000–200 cm^{-1} and UV/visible spectra as powdered solids diluted with $BaSO_4$, using a Jasco V670 spectrophotometer with a 60 mm integrating sphere. ^{1}H and $^{13}C\{^{1}H\}$ NMR spectra were recorded from CD_2Cl_2 or $CDCl_3$ solutions using a Bruker AV II 400 spectrometer and are referenced to the residual protio-solvent resonance. $^{77}Se\{^{1}H\}$ NMR spectra were recorded using a Bruker AV II 400 spectrometer and are referenced to external neat $SeMe_2$. Microanalyses on new complexes were performed by London Metropolitan University. Preparations used standard Schlenk and glove box techniques under a N_2 atmosphere with rigorous exclusion of moisture. Solvents were dried by distillation from CaH_2 (CH_2Cl_2) or Na/benzophenone ketyl (diethyl ether, toluene, n-hexane).

The $NbCl_5$, $TaCl_5$ Me_2S and $^{n}Bu_2S$ were obtained from Aldrich and used as received. Me_2Se was obtained from Strem. $^{n}Bu_2Se$ and the dithio- and diselenoethers were made by literature methods or minor modifications thereof [22].

2.1 [$Nb_2Cl_4(Me_2S)_2(\mu\text{-}Cl)_2(\mu\text{-}Me_2S)$]

Prepared by the literature method [16,23]. Dark purple solid. Yield: 85%. *Anal.* calc. for $C_6H_{18}Cl_6Nb_2S_3$ (584.9): C, 12.3; H, 3.1. Found: C, 12.4; H, 3.0%. ^{1}H NMR ($CDCl_3$, 298 K): δ 2.64 (s, [12H], terminal Me_2S), 3.35 (s, [6H], bridging Me_2S). $^{13}C\{^{1}H\}$ NMR ($CDCl_3$, 298 K): δ 22.69 (terminal Me_2S), 30.03 (bridging Me_2S). IR (Nujol): ν = 345s, 330s, 315s (Nb–Cl) cm^{-1}. UV/vis (d.r.)/cm^{-1}: 5170, 5800, 5950, 7220, 8585, 13440, 18550, 25800, 32470.

2.2 [$Nb_2Cl_4(^{n}Bu_2S)_2(\mu\text{-}Cl)_2(\mu\text{-}^{n}Bu_2S)$]

Magnesium turnings (0.071 g, 2.5 mmol) and $NbCl_5$ (0.267 g, 1.0 mmol) were added to anhydrous CH_2Cl_2 (5 mL). A solution of $^{n}Bu_2S$ (0.45 mL, 2.5 mmol) in Et_2O (0.7 mL, 2.5 mmol) was then added with stirring. The colour changed to red-brown immediately and after stirring for 2 h, the colour had become purple. The mixture was stirred for a further 12 h at room temperature, filtered and the solvent was removed *in vacuo*, leaving a sticky purple solid. This solid was stirred with n-hexane (3 mL) and the dark purple solid produced filtered off and dried *in vacuo*. The filtrate was refrigerated and purple crystals formed after 2 weeks. Combined isolated yield of solid and crystals: 0.113 g, 27%. *Anal.* calc.

for $C_{24}H_{54}Cl_6Nb_2S_3$ (837.13): C, 34.4; H, 6.5. Found: C, 34.3; H, 6.6%. ^{1}H NMR ($CDCl_3$, 298 K): δ 0.94-0.98 (m, [18H], Me), 1.44-1.50 (m, [12H], C<u>H</u>$_2$Me), 1.69-1.83 (m, [8H], terminal-SCH$_2$C<u>H</u>$_2$), 1.86-2.08 (m, [4H], bridging-SCH$_2$C<u>H</u>$_2$), 3.04 (t, [8H], terminal-SCH$_2$), 3.59-3.75 (m, [4H], bridging-SCH$_2$). ^{13}C{^{1}H} NMR ($CDCl_3$, 298 K): δ 13.60 (Me, terminal ^{n}Bu$_2$S), 13.76 (Me, bridging ^{n}Bu$_2$S), 21.91 (<u>C</u>H$_2$Me, terminal ^{n}Bu$_2$S), 22.37 (<u>C</u>H$_2$Me, bridging ^{n}Bu$_2$S), 28.66 (SCH$_2$<u>C</u>H$_2$, bridging ^{n}Bu$_2$S), 30.69 (SCH$_2$<u>C</u>H$_2$, terminal ^{n}Bu$_2$S, 36.53 (SCH$_2$, terminal ^{n}Bu$_2$S, 41.45 (SCH$_2$, bridging ^{n}Bu$_2$S. IR (Nujol): ν = 349m, 327m (Nb–Cl) cm^{-1}. UV/vis (d.r.)/cm^{-1}: 5155, 5190, 5750, 7220, 8510, 11350, 13160, 18018, 26110(sh), 33900.

2.3 [$Ta_2Cl_4(Me_2S)_2(\mu$-$Cl)_2(\mu$-$Me_2S)$]

Magnesium (0.56 g, 23 mmol) and $TaCl_5$ (4.8 g. 13 mmol) were added to toluene (150 mL), followed by Me_2S (2 mL) when a green solution formed. Diethyl ether (20 mL) was then added and after 10 min, the solution turned brown, and was then stirred for 3 days. The dark brown solution was filtered, and the filtrate was reduced to 20 mL *in vacuo.* n-Hexane (20 mL) was added and the solid produced filtered off and dried *in vacuo*. Yield: 1.79 g, 36%. *Anal.* calc. for $C_6H_{18}Cl_6S_3Ta_2$ (761.02): C, 9.5; H, 2.3. Found: C, 9.5; H, 2.3%. ^{1}H NMR ($CDCl_3$, 298 K): δ 2.74 (s, [12H], SMe terminal), 3.48 (s, [6H], SMe bridging). ^{13}C{^{1}H} NMR ($CDCl_3$): 22.94 (terminal Me_2S), 40.88 (bridging Me_2S). IR (Nujol): ν = 329s, 314s (Ta–Cl) cm^{-1}. UV/vis (d.r.)/cm^{-1}: 5140, 5800, 5970, 7200, ~9500(sh), 10600, 14925, 20660, 28900sh, ~33000, 39400.

2.4 [$Ta_2Cl_4(^nBu_2S)_2(\mu$-$Cl)_2(\mu$-$^nBu_2S)$]

Magnesium (0.56 g, 23 mmol) and $TaCl_5$ (4.8 g, 13.4 mmol) was added to toluene (50 mL). ^{n}Bu$_2$S (1.2 mL, 13.4 mmol) was added and the colour changed to light yellow. After 30 min, diethyl ether (20 mL) was added and the solution was stirred for 2 days, turning red. After filtering, the solvent was removed *in vacuo,* leaving sticky red solid. This was dissolved in n-hexane (10 mL) and placed in the freezer (−18 °C). After 24 h, deep red crystals had formed. Yield: 4.65 g, 69%. *Anal.* calc. for $C_{24}H_{54}Cl_6S_3Ta_2$ (1013.22): C, 28.4; H, 5.4. Found: C, 28.4; H, 5.3%. ^{1}H NMR ($CDCl_3$, 298 K): δ 0.96 (t, [12H], Me, terminal ^{n}Bu$_2$S), 1.02 (t, [6H], Me, bridging ^{n}Bu$_2$S), 1.45-1.52 (m, [8H], C<u>H</u>$_2$Me, terminal ^{n}Bu$_2$S), 1.55-1.60 (m, [4H], C<u>H</u>$_2$Me, bridging ^{n}Bu$_2$S), 1.75-1.79 (m, [8H], SCH$_2$C<u>H</u>$_2$, terminal ^{n}Bu$_2$S), 2.10-2.14 (m, [4H], SCH$_2$C<u>H</u>$_2$, bridging ^{n}Bu$_2$S), 3.12 (t, [8H], SCH$_2$, terminal ^{n}Bu$_2$S), 3.73-3.77 (m, [4H], SCH$_2$, bridging ^{n}Bu$_2$S). ^{13}C{^{1}H} NMR ($CDCl_3$, 298 K): δ 13.60 (Me, terminal ^{n}Bu$_2$S), 14.01 (Me, bridging ^{n}Bu$_2$S), 21.89 (<u>C</u>H$_2$Me, terminal ^{n}Bu$_2$S), 23.13 (<u>C</u>H$_2$Me, bridging ^{n}Bu$_2$S), 29.35 (SCH$_2$<u>C</u>H$_2$, bridging ^{n}Bu$_2$S), 30.78 (SCH$_2$<u>C</u>H$_2$, terminal ^{n}Bu$_2$S,) 36.75 (SCH$_2$, terminal ^{n}Bu$_2$S), 52.37 (SCH$_2$, bridging

$^{n}Bu_2S$). IR (Nujol): ν = 325s, 317sh (Ta–Cl) cm^{-1}. UV/vis (d.r.)/cm^{-1}: 5100, 5760, 5870, 6850, 7200, ~9100(sh), 10250, 14500, 19760, 27550, 40150.

2.5 $[Ta_2Cl_6(Me_2S)_2(\mu\text{-}Cl)_2]$

The reaction was carried out as in *2.3* above, but with a shorter reaction time (~36 h) and after removing the $[Ta_2Cl_4(Me_2S)_2(\mu\text{-}Cl)_2(\mu\text{-}Me_2S)]$, the filtrate was refrigerated. This produced a mixture of brown and orange crystals. The latter were identified as compound *2.5* by an X-ray crystal structure. ^1H NMR ($CDCl_3$, 298 K): δ 3.15 (s, SMe). IR (Nujol): ν = 366s, 350s (Ta–Cl) cm^{-1}.

2.6 $[Nb_2Cl_4(MeSCH_2CH_2SMe)_2(\mu\text{-}Cl)_2]$

$[Nb_2Cl_4(Me_2S)_2(\mu\text{-}Cl)_2(\mu\text{-}Me_2S)]$ (0.29 g, 0.5 mmol) was dissolved in toluene (10 mL). $MeSCH_2CH_2SMe$ (0.368 g, 1.6 mmol) in toluene (7 mL) and then added with stirring. After 3 days, the pink solid was collected by filtration, washed three times with n-hexane (10 mL) and dried *in vacuo*. Pink powder. Yield: 0.178 g, 57%. *Anal.* calc. for $C_8H_{20}Cl_6Nb_2S_4$ (643.03): C, 14.9; H, 3.1. Found: C, 14.9; H, 3.3%. ^1H NMR (CD_2Cl_2, 298 K): δ 2.23 (s, [12H], SMe), 2.78 (br s, [8H], CH_2). IR (Nujol): ν = 346sh, 338s, 293m (Nb–Cl) cm^{-1}. UV/vis (d.r.)/cm^{-1}: 5173, 5230, 6215, 7205, 8330(sh), 9900(sh), 19530, 32260, 38515.

2.7 $Ta_2Cl_4(Me_2S)_4(\mu\text{-}S)_2]$

Prepared as in [18]. $[Ta_2Cl_4(Me_2S)_2(\mu\text{-}Cl)_2(\mu\text{-}Me_2S)]$ (0.15 g, 0.2 mmol) was dissolved in toluene (10 mL) and Me_2S (1 mL, 13.6 mmol) was added and the reaction mixture was stirred for 1 h. Some solids remained and were removed by filtration. The solution was carefully layered with Me_2S_2 (0.015 mL, 0.17 mmol) in hexane (10 mL) and left undisturbed. After 2 weeks, some red crystals had formed, together with some greenish powder. The crystals were separated manually under N_2 and washed with pentane. Yield of red crystals: 0.018 g, 11%. *Anal.* calc. for $C_8H_{24}Cl_4S_6Ta_2$ (816.37): C, 11.8; H, 3.0%. Found: C, 11.9; H, 2.9%. ^1H NMR (CD_2Cl_2, 298 K): insoluble. IR (Nujol): ν = 320s, 295m (Ta–Cl) cm^{-1}.

2.8 $[Nb_2Cl_4(MeSeCH_2CH_2SeMe)_2(\mu\text{-}Cl)_2]$

$[Nb_2Cl_4(Me_2S)_2(\mu\text{-}Cl)_2(\mu\text{-}Me_2S)]$ (0.238 g, 0.41 mmol) in toluene (15 mL) and $MeSeCH_2CH_2SeMe$ (0.384 g, 1.8 mmol) in toluene (2 mL) were combined with stirring. The solution was stirred for 20 h, during which time a purple solid precipitated. This was filtered off, washed twice with n-hexane (20 mL) and dried *in vacuo*, leaving a purple powder. Yield: 0.230 g, 68%. *Anal.* Calc. for $C_8H_{20}Cl_6Nb_2Se_4$ (830.61): C, 11.6; H, 2.4. Found: C, 11.6; H, 2.4%. ^1H NMR (CD_2Cl_2, 298 K): δ 2.17 (s, [12H], Me),

3.0 (s, [8H], CH_2). $^{77}Se\{^1H\}$ NMR (CD_2Cl_2, 295 K): δ 267 (s, Me_2Se_2 see text). IR (Nujol): ν = 359m, 315m, 286m (Nb–Cl) cm^{-1}. UV/vis (d.r.)/cm^{-1}: 5320, 7240, ~8330. ~10280, 19490, 29675, 39000(sh).

2.9 [$Nb_2Cl_4(MeSeCH_2CH_2CH_2SeMe)_2(\mu\text{-}Cl)_2$]

This complex was synthesised as for 2.8, using $MeSeCH_2CH_2CH_2SeMe$, giving the product as a light purple powder. Yield: 49%. *Anal.* Calc for $C_{10}H_{24}Cl_6Nb_2Se_4$ (858.7): C, 14.0; H, 2.8. Found: C, 14.1; H, 2.8%. The product dissolves in CD_2Cl_2 or MeCN, but the solution rapidly darkens to brown preventing ^1H NMR studies. IR (Nujol): ν = 342s, 325m (Nb–Cl) cm^{-1}. UV/vis (d.r.)/cm^{-1}: 5445, 5810, 5970, 7230, 8920, ~9600(sh), 18730, 29850, 36000.

2.10 [$Ta_2Cl_4(MeSeCH_2CH_2SeMe)_2(\mu\text{-}Cl)_2$]

[$Ta_2Cl_4(Me_2S)_2(\mu\text{-}Cl)_2(\mu\text{-}Me_2S)$] (0.200 g, 0.26 mmol) was dissolved in toluene (20 mL) and $MeSeCH_2CH_2SeMe$ (0.34 g, 1.6 mmol) was added. The reaction mixture was stirred for 36 h, producing a brown powder. This was filtered off, washed with n-hexane (40 mL) and dried in *vacuo*. Yield: 0.19 g, 73%. *Anal.* calc. for $C_8H_{20}Cl_6Se_4Ta_2$ (1006.70): C, 9.5; H, 2.0. Found: C, 9.6; H, 1.9%. ^1H NMR (CD_2Cl_2, 295 K): δ 2.31 (s, [12H], Me), 2.76 (s, [8H], CH_2). $^{77}Se\{^1H\}$ NMR (CD_2Cl_2, 295 K): δ 265 (s, Me_2Se_2 see text). IR (Nujol): ν = 322br, 289sh (Ta–Cl) cm^{-1}. UV/vis (d.r.)/cm^{-1}: 5165, 5790, 5930, 7220, 9615, 13900, 17950, 26955(sh), 30960(sh), 38910.

2.11 [$Ta_2Cl_4(^nBuSeCH_2CH_2CH_2Se^nBu)_2(\mu\text{-}Cl)_2$]

was prepared similarly to *2.10* as a brown powder using $^nBuSeCH_2CH_2CH_2Se^nBu$. Yield: 22%. *Anal.* calc. for $C_{22}H_{48}Cl_6Se_4Ta_2$ (1203.1): C, 22.0; H, 4.0. Found: C, 21.7; H, 4.0%. IR (Nujol): ν = 329 vbr, 295sh cm^{-1}. A few crystals of [$\{Ta_2Cl_4(\mu\text{-}Cl)_2(\mu\text{-}SMe_2)\}_2(\mu\text{-}^nBuSeCH_2CH_2CH_2Se^nBu)_2$] were obtained from the filtrate from the synthesis, by vapour diffusion of hexane into a toluene solution.

2.12 [$Ta_2Cl_4\{o\text{-}C_6H_4(CH_2SeMe)_2\}_2(\mu\text{-}Se)_2$]

[$\{Ta_2Cl_6(Me_2S)_2(\mu\text{-}Cl)_2(\mu\text{-}Me_2S)$] (0.1 g, 0.13 mmol) was dissolved in toluene (20 mL) at room temperature, *o*-$C_6H_4(CH_2SeMe)_2$ (0.146 g, 0.5 mmol) in toluene (2 mL) was then added and the reaction mixture was left to stir for 5 h. Some pale brown-green solid was removed by filtration (0.15 g). The remaining brown filtrate was then layered with hexane, giving a few yellow-orange crystals which were shown by single crystal X-ray analysis to be [$Ta_2Cl_4\{o\text{-}C_6H_4(CH_2SeMe)_2\}_2(\mu\text{-}Se)_2$].

2.13 X-Ray Experimental.

Details of the crystallographic data collection and refinement parameters are given in Table 1. Crystals suitable for single crystal X-ray analysis were obtained as described above. Data collections used a Rigaku AFC12 goniometer equipped with an enhanced sensitivity (HG) Saturn724+ detector mounted at the window of an FR-E+ SuperBright molybdenum (λ = 0.71073) rotating anode generator with VHF Varimax optics (70 micron focus) with the crystal held at 100 K (N_2 cryostream). Structure solution and refinements were performed using SHELX(S/L)97 or SHELX-2013 [24] and were mostly straightforward, except where detailed below. H atoms bonded to C were placed in calculated positions using the default C-H distance and refined using a riding model. [{$Ta_2Cl_4(\mu\text{-}Cl)_2(\mu\text{-}Me_2S)$}$_2$($\mu$-^{n}BuSeCH$_2CH_2CH_2$Se^{n}Bu)$_2$]: this was a small, weakly diffracting crystal and refinement revealed disorder in the butyl chains which could not be modelled satisfactorily using split C atom occupancies, hence these atoms were refined isotropically. [{$Nb_2Cl_4(\mu\text{-}Cl)_2(\mu\text{-}Me_2S)$}$_2$($\mu$-MeSeCH$_2CH_2CH_2$SeMe)$_2$]: this was a small, weakly diffracting crystal, and during refinement disorder was evident in the C atoms of the bridging selenoether, hence these were refined isotropically. These two structures serve to confirm the identity of the complex and the connectivities, but detailed analysis of bond distances and angles are not warranted. In some of the crystals significant residual electron density peaks close to the heavy atoms (Ta or Nb) were observed, attributed to imperfect absorption correction, as indicated in the comments in the cif files. Crystallographic data in cif format have been deposited with the Cambridge Crystallographic Data Centre (CCDC) and given numbers 1409136-1409143. Copies of the data can be obtained free of charge from The Director, CCDC, 12 Union Road, Cambridge, CB2 1EZ, UK, fax: +44 1223 366033, e-mail: deposit@ccdc.cam.ac.uk or on the web at http://www.ccdc.cam.ac.uk .

3. Results and Discussion

3.1 The [$M_2Cl_4(Me_2S)_2(\mu\text{-}Cl)_2(\mu\text{-}Me_2S)$] were prepared by literature methods [16,23] which involve the reduction of the corresponding MCl_5 with magnesium metal in toluene/diethyl ether solution. Complexes of dimethylchalcogenides are not well suited as CVD reagents, because they lack the β-hydride decomposition route [11,12,13], and hence the new complexes [$M_2Cl_4(^nBu_2S)_2(\mu\text{-}Cl)_2(\mu$-$^nBu_2S)$] were prepared by an analogous method (Scheme 1). X-Ray structures of both complexes were determined (Figures 1 and 2) which showed them to be isomorphous and confirmed the expected confacial bioctahedral geometries, as found for the Me_2S complexes [15,17], and the corresponding bond lengths and angles are not significantly different.

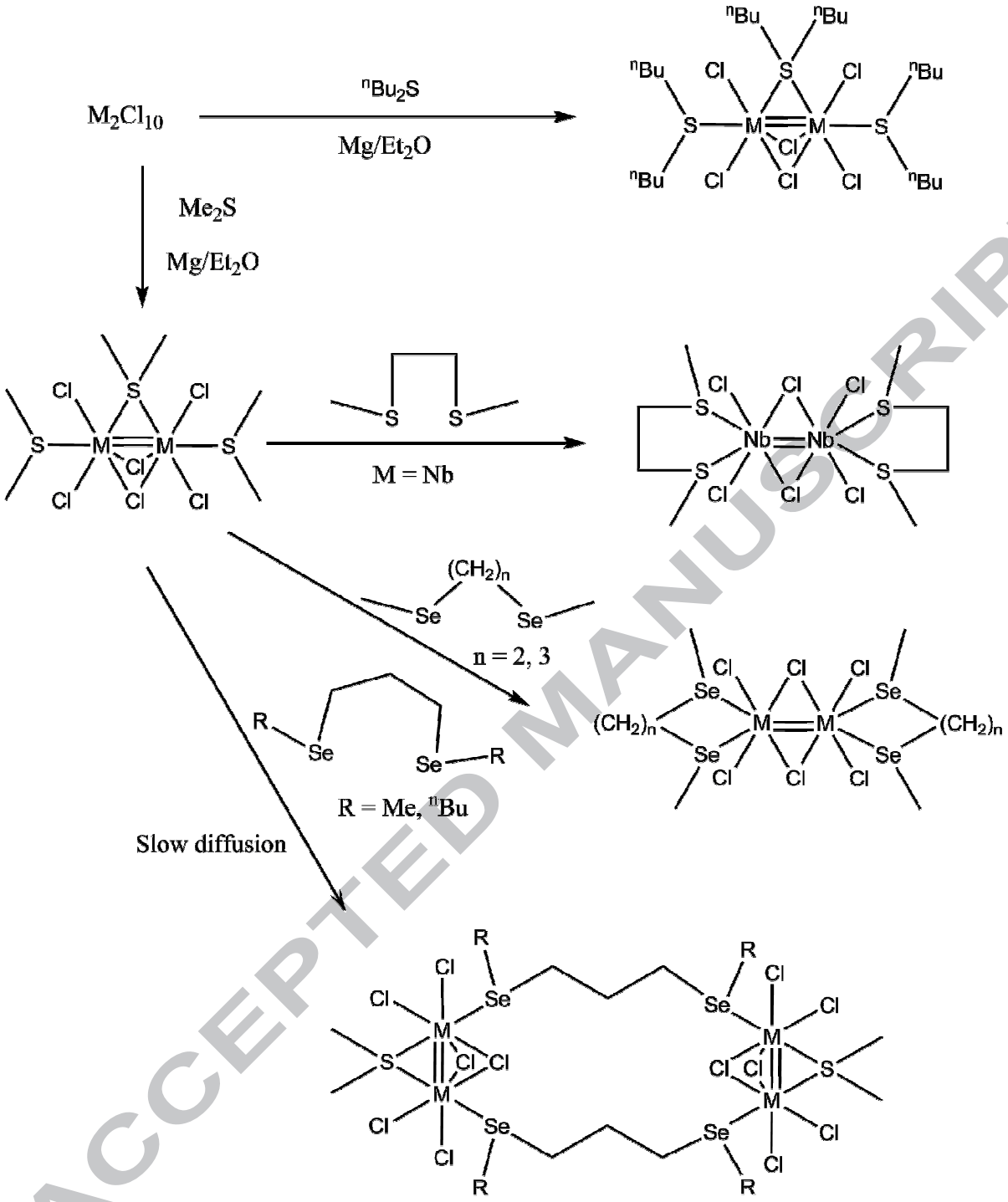

Scheme 1. Some reactions of the dinuclear Nb and Ta thioethers in this work

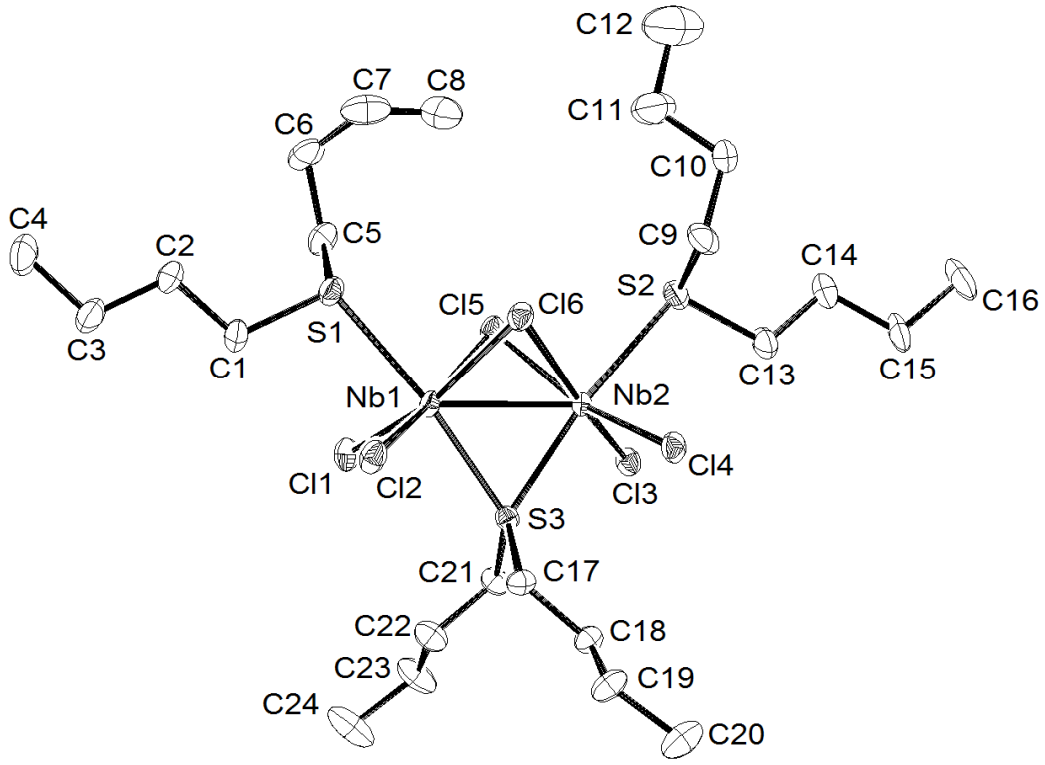

Figure 1. Structure of one of the two crystallographically independent $[Nb_2Cl_4(^nBu_2S)_2(\mu\text{-}Cl)_2(\mu\text{-}^nBu_2S)]$ molecules in the asymmetric unit, showing the atom numbering scheme and with ellipsoids drawn at the 50% probability level. The second dimer has crystallographic C_2 symmetry, but is otherwise similar. Hydrogen atoms are omitted for clarity, and there is some disorder in the ^{n}Bu chains (not shown). Selected bond lengths (Å) and angles (°): Nb1–S3 = 2.4211(14), Nb1–S1 = 2.6410(15), Nb2–S3 = 2.4167(14), Nb2–S2 = 2.6519(15), Nb1–Cl1 = 2.3906(17), Nb1–Cl2 = 2.3783(14), Nb2–Cl3 = 2.3872(14), Nb2–Cl4 = 2.3849(16), Nb2–Cl5 = 2.4912(15), Nb1–Cl5 = 2.5221(14), Nb1–Cl6 = 2.5011(16), Nb2–Cl6 = 2.5160(14), Nb1–Nb2 = 2.7027(8), Nb2–Cl5–Nb1 = 65.24(4), Nb1–Cl6–Nb2 = 65.19(4), Nb2–S3–Nb1 = 67.93(4).

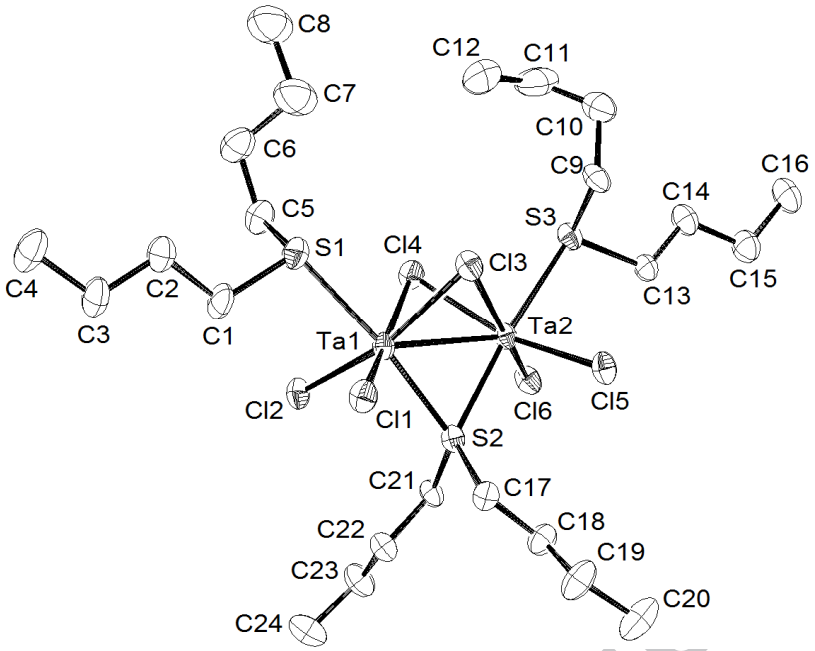

Figure 2. Structure of one of the molecules of $[Ta_2Cl_4(^nBu_2S)_2(\mu\text{-}Cl)_2(\mu\text{-}^nBu_2S)]$ showing the atom numbering scheme and with ellipsoids drawn at the 50% probability level. Hydrogen atoms are omitted for clarity, and only one arrangement of the disordered Bu chains is shown. The second dimer has crystallographic C_2 symmetry, but is otherwise similar. Selected bond lengths (Å) and angle (°): Ta1–Cl1 = 2.3927(14), Ta1–Cl2 = 2.3987(14), Ta1–S2 = 2.4026(16), Ta1–Cl3 = 2.5118(15), Ta1–Cl4 = 2.5346(15), Ta1–S1= 2.6581(17), Ta2–Cl6 = 2.3881(14), Ta2–Cl5 = 2.3934(15), Ta2–S2 = 2.4077(16), Ta2–Cl4 = 2.5172(15), Ta2–Cl3 = 2.5331(14), Ta2–S3 = 2.6532(16), Ta1–Ta2 = 2.7103(3), Ta1–Cl3–Ta2 = 64.99(4), Ta2–Cl4–Ta1 = 64.89(4), Ta1–S2–Ta2 = 68.59(5).

The major notable features are the acute angles at the bridging atoms M–Y–M (Y = S or Cl) of 65–69°, and that whilst the terminal M–Cl bonds are shorter than the bridging M–Cl, the reverse is true for the terminal and bridging sulfurs, which may reflect some π-repulsion from the "free" lone pair on the terminal thioether groups on the relatively electron rich metal(III) centres. The compounds are diamagnetic, consistent with formal double bonds derived from M^{III}=M^{III} configuration. In a confacial bi-octahedron of type $[M_2X_9]$, with all X groups the same, the M–M bonding is described as one σ and two "π/δ" bonds [25]. In the lower symmetry in the present complexes, the degeneracy of the two π/δ orbitals is lifted, resulting in a diamagnetic ground state (σ^2 π/δ^2 π/δ^0), and this is supported by the observed bond lengths [15-18]. The structure of $[Ta_2Cl_4(Me_2S)_2(\mu\text{-}Cl)_2(\mu\text{-}Me_2S)]$ was reported by Cotton and Najjar [15] in the space group Pnma with the methyl groups on the terminal Me_2S ligands pointing in the same direction. We obtained crystals of a polymorph in space group Pbcn, with the

molecules having an additional C_2 axis resulting from the terminal S–Me groups pointing in different directions (Figure 3). As expected, the dimensions differ little between the two structures.

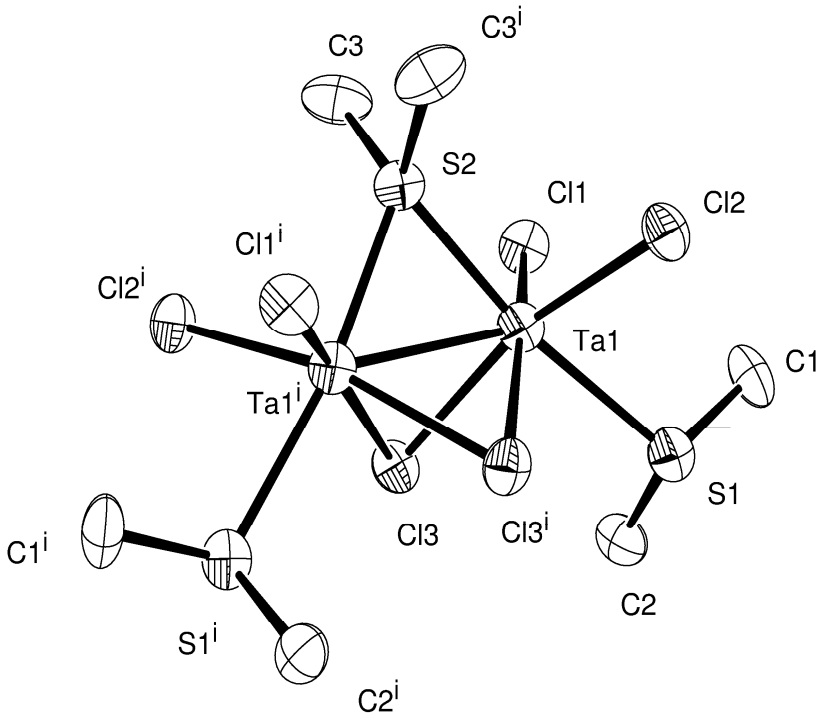

Figure 3. Structure of the Pbcn polymorph of $[Ta_2Cl_4(Me_2S)_2(\mu\text{-}Cl)_2(\mu\text{-}Me_2S)]$ showing the atom numbering scheme. Ellipsoids drawn at the 50% probability level. Hydrogen atoms are omitted for clarity. Selected bond lengths (Å) and angles (°): Ta1–Cl1 = 2.348(5), Ta1–Cl2 = 2.371(5), Ta1–S2 = 2.373(7), Ta1–Cl3 = 2.507(5), Ta1–$Cl3^i$ = 2.512(5), Ta1–S1 = 2.617(6), Ta1–$Ta1^i$ = 2.664(2), Ta1–Cl3–$Ta1^i$ = 64.13(13), Ta1–S2–$Ta1^i$ = 68.3(2).

The spectroscopic data on these four complexes are unexceptional, but clearly fingerprint them as analogues. The UV/visible spectra of the solids (diffuse reflectance samples diluted with $BaSO_4$) (Figure 4(a)) show a complex pattern of absorptions and a detailed assignment is not possible due to the band overlaps and low symmetry. However, the very weak features < 8000 cm^{-1} probably involve electron rearrangements within the M_2 bonding orbitals [25], the more intense features between ~10000 and 20000 cm^{-1} transitions between the bonding and anti-bonding orbitals with predominantly metal character, whilst the higher energy bands will be mainly charge transfer L→M in origin.

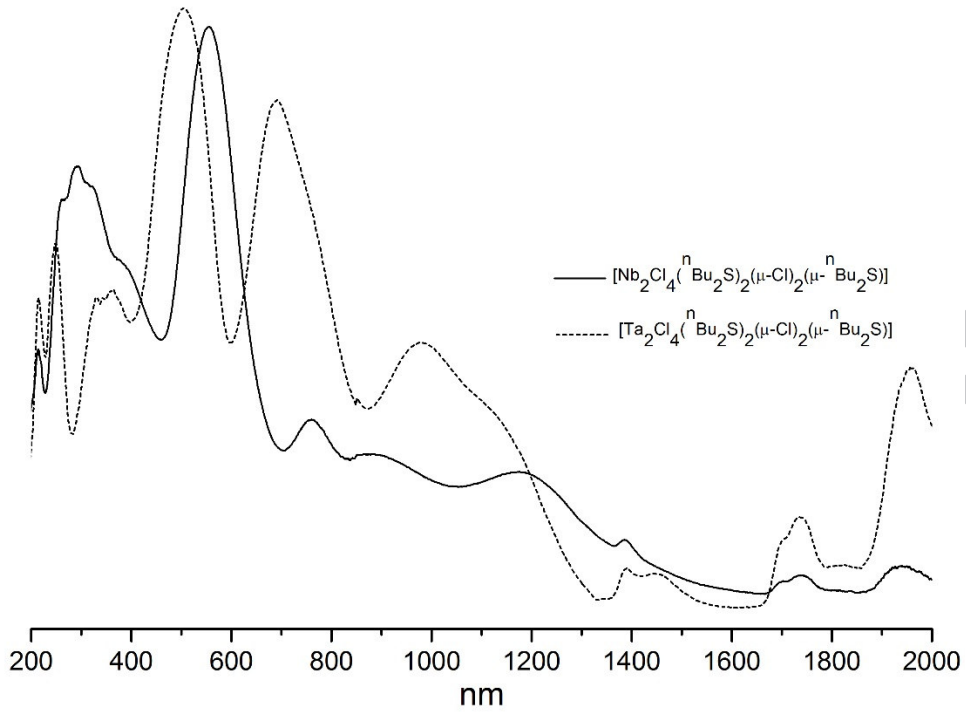

(a)

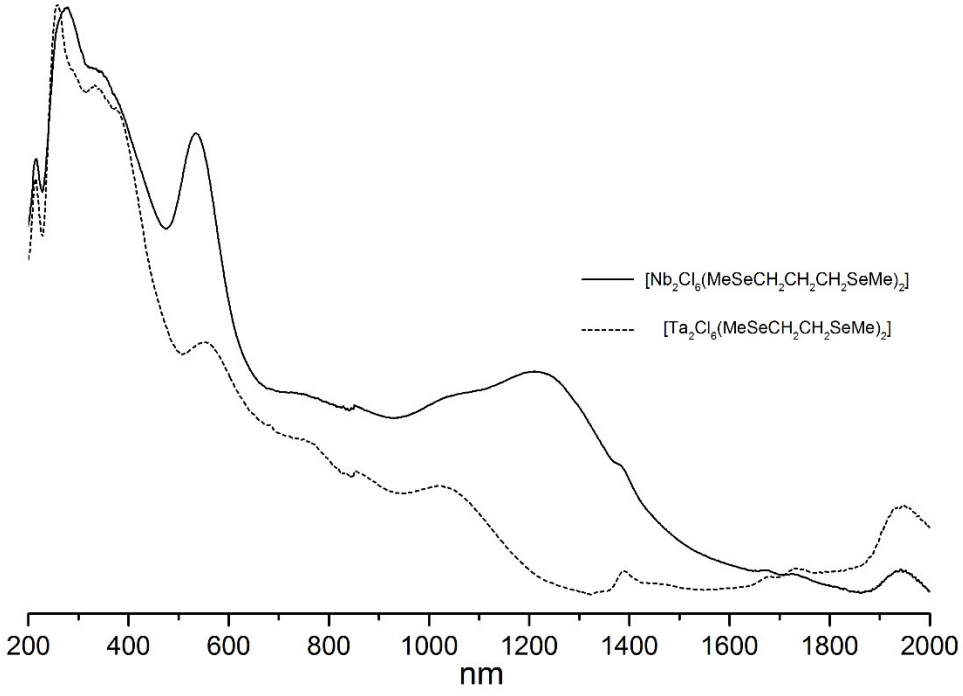

(b)

Figure 4. (a) UV/visible spectra of solid $[M_2Cl_4(^nBu_2S)_2(\mu\text{-}Cl)_2(\mu\text{-}^nBu_2S)]$ (M = Nb and Ta) and (b) $[M_2Cl_6(MeSeCH_2)_nSeMe)_2]$.

Although Matsuura *et. al.* [16] reported a high yield of $[Nb_2Cl_4(Me_2Se)_2(\mu\text{-}Cl)_2(\mu\text{-}Me_2Se)]$ by reduction of $NbCl_5/Me_2Se$ with Mg in CH_2Cl_2/Et_2O, despite many attempts to replicate the synthesis, we have been unable to obtain this compound or the tantalum analogue, instead obtaining intractable mixtures, probably due to C–Se cleavage. The metathesis of $[Nb_2Cl_4(Me_2S)_2(\mu\text{-}Cl)_2(\mu\text{-}Me_2S)]$ with Me_2Se is reported to give $[Nb_2Cl_4(Me_2Se)_2(\mu\text{-}Cl)_2(\mu\text{-}Me_2S)]$, although an X-ray structure of a crystal from this preparation showed the composition to be in fact $[Nb_2Cl_6(Me_2Se)_{1.3}(Me_2S)_{1.7}]$, with disordered terminal chalcogenoethers [17].

3.2 Ta_2^{8+} dimers

As noted in the Introduction, small changes in the experimental conditions can result in impure products, or even mixtures of complexes, reinforcing the need to critically evaluate the data on each batch of material. As an example of this, one synthesis of brown $[Ta_2Cl_4(Me_2S)_2(\mu\text{-}Cl)_2(\mu\text{-}Me_2S)]$ was carried out with a shorter reaction time, 36 h instead of 72 h. After removal of the solid $[Ta_2Cl_4(Me_2S)_2(\mu\text{-}Cl)_2(\mu\text{-}Me_2S)]$, the filtrate was refrigerated and produced a mixture of brown and orange crystals. The latter exhibited only one methyl resonance in the ^1H NMR spectrum compared to two in the brown bulk material, and had Ta–Cl IR stretches at higher frequency. The X-ray structure showed the orange crystals to contain the Ta_2^{8+} $[Ta_2Cl_6(Me_2S)_2(\mu\text{-}Cl)_2]$ with edge-bridging chlorides (Figure 5). The Ta–Ta interaction is now a single σ bond and, at 3.051(3) Å, is significantly longer than the double bonds in the Ta_2^{6+} dimers above. However, whilst the terminal Ta–S and Ta–Cl bond lengths in the two series of dimers show some dependence upon the *trans* ligands, the effect of formal oxidation state is not significant and hence the Ta–S and Ta–Cl bond lengths do not clearly distinguish the tantalum oxidation state.

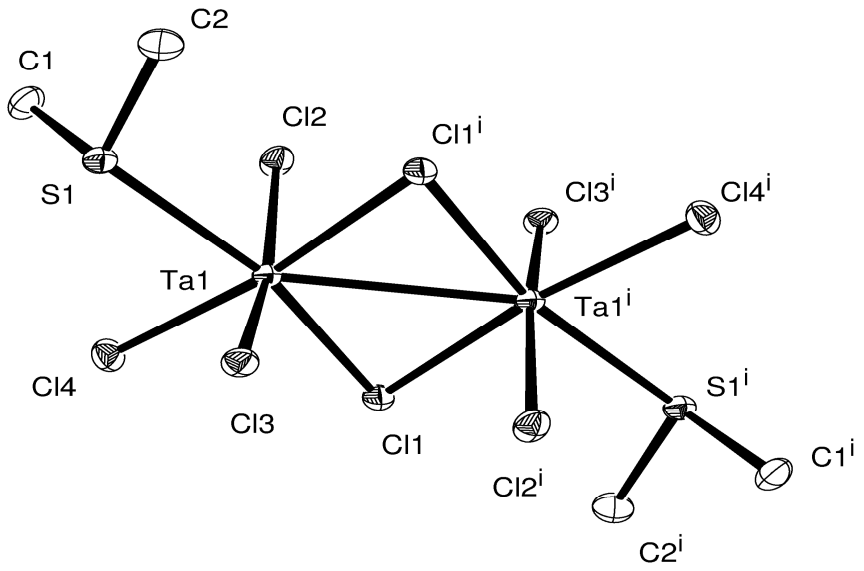

Figure 5. The structure of $[Ta_2Cl_6(Me_2S)_2(\mu\text{-}Cl)_2]$ showing the atom numbering scheme and with ellipsoids drawn at the 50% probability level. Hydrogen atoms are omitted for clarity. Selected bond lengths (Å) and angles (°): Ta1–Cl3 = 2.320(2), Ta1–Cl2 = 2.321(3), Ta1–Cl4 = 2.3881(17), Ta1–Cl1 = 2.4208(17), Ta1–Cl1^i = 2.5011(18), Ta1–S1 = 2.620(2), Ta1–Ta1^i = 3.051(3), Ta1–Cl1–Ta1 = 76.60(7).

A poor yield (11%) of red crystals were deposited from reaction of $[Ta_2Cl_4(Me_2S)_2(\mu\text{-}Cl)_2(\mu\text{-}Me_2S)]$ with Me_2S_2 and excess Me_2S in toluene/hexane solution after 2 weeks. These were identified as $[Ta_2Cl_4(Me_2S)_4(\mu\text{-}S)_2]$ by an X-ray study, with the Ta_2^{8+} core confirmed by the long Ta–Ta bond of 2.8368(3) Å. The structure is the same as that reported by Canich and Cotton [18], who formulated it as $[Ta_2Cl_4(Me_2S)_4(\mu\text{-}Cl)_2]$, and which was subsequently reformulated as $[Ta_2Cl_4(Me_2S)_4(\mu\text{-}S)_2]$ by Babaian-Kibala *et. al.* [21]. Our data are in good agreement with the published structure, allowing for the different temperature of data collection (295 K [18] *versus* 100 K) (see Supplementary data).

3.3 Dithioether and diselenoether adducts of M_2^{6+}

The reaction of $[Nb_2Cl_4(Me_2S)_2(\mu\text{-}Cl)_2(\mu\text{-}Me_2S)]$ with $MeSCH_2CH_2SMe$ in toluene gave the red complex $[Nb_2Cl_4(MeSCH_2CH_2SMe)_2(\mu\text{-}Cl)_2]$ and using 2,5-diselenahexane, the corresponding $[Nb_2Cl_4(MeSeCH_2CH_2SeMe)_2(\mu\text{-}Cl)_2]$ formed. In freshly prepared CD_2Cl_2 solution, each complex shows singlet CH_3 and CH_2 ^{1}H NMR resonances, to high frequency of the parent ligand. On cooling

the solutions to 190 K, the CH_3 resonances split into two of unequal intensity, assigned to *meso* and *DL* isomers of the chelating bidentate ligand, which are resolved as the rate of pyramidal inversion at the E atom slows [26]; the original singlet resonances are restored on re-warming the solution. The solutions darken over time, with the selenium-containing complexes depositing a brown solid and leaving a colourless solution after ~ 24 h. The ^{77}Se NMR spectra of the colourless solutions show only a singlet resonance in each complex at δ = 265, which can be assigned to Me_2Se_2 [27], resulting from ligand fragmentation. The poor solubility and relative insensitivity of the ^{77}Se nucleus prevented spectra being obtained of the initial complexes. Cleavage of C–Se bonds in diselena-alkanes occurs with some other early transition metal systems [28], and other examples with Nb/Ta are described below. A pink $[Nb_2Cl_4(MeSeCH_2CH_2CH_2SeMe)_2(\mu\text{-}Cl)_2]$ was also isolated, but this was very unstable in CH_2Cl_2 solution, preventing solution spectroscopic measurements, and other complexes with this ligand were not pursued. The reaction of $[Ta_2Cl_4(Me_2S)_2(\mu\text{-}Cl)_2(\mu\text{-}Me_2S)]$ with $MeSeCH_2CH_2SeMe$ gave a brown $[Ta_2Cl_4(MeSeCH_2CH_2SeMe)_2(\mu\text{-}Cl)_2]$. The IR and UV/visible (Figure 4(b) spectra of these complexes indicate they are close analogues of the related Nb systems, and they are formulated as M_2^{6+} edge-shared dimers (chloride-bridged) containing with $\sigma^2\pi^2\delta^0$ M=M bonds [25]. This formulation of the niobium dimers and $[Ta_2Cl_4(MeSeCH_2CH_2SeMe)_2(\mu\text{-}Cl)_2]$ as edged-shared bi-octahedral M_2^{6+} entities follows from their similar UV-visible spectra and by analogy with the literature structure of $[Nb_2Cl_4(EtSCH_2CH_2SEt_2(\mu\text{-}Cl)_2]$ [18,21]. Several attempts to isolate a pure complex from the reaction of 2,5-dithiahexane and $[Ta_2Cl_4(Me_2S)_2(\mu\text{-}Cl)_2(\mu\text{-}Me_2S)]$ were unsuccessful.

A number of other selenium containing ligands were explored in this work in attempts to improve yields or solution solubility/stability. Most gave intractable mixtures of complexes or poorly reproducible results and only three reactions merit mention. In an attempt to improve solubility in chlorocarbons, the complex $[Ta_2Cl_4(^nBuSeCH_2CH_2CH_2Se^nBu)_2(\mu\text{-}Cl)_2]$ was prepared in poor yield using $^nBuSeCH_2CH_2CH_2Se^nBu$ in place of $MeSeCH_2CH_2SeMe$. Layering of the toluene filtrate from this reaction with hexane produced a few crystals which were identified as the "dimer of dimers", $[\{Ta_2Cl_4(\mu\text{-}Cl)_2(\mu\text{-}Me_2S)\}_2(\mu\text{-}^nBuSeCH_2CH_2CH_2Se^nBu)_2]$ (Figure 6). The molecule is a Ta_2^{6+} complex, most clearly shown by the Ta–Ta bond length of 2.6802(16) Å, which is in excellent agreement with those reported above for $[Ta_2Cl_4(R_2S)_2(\mu\text{-}Cl)_2(\mu\text{-}R_2S)]$. This species clearly assembles by replacing the terminal Me_2S groups by the bridging diselenoethers.

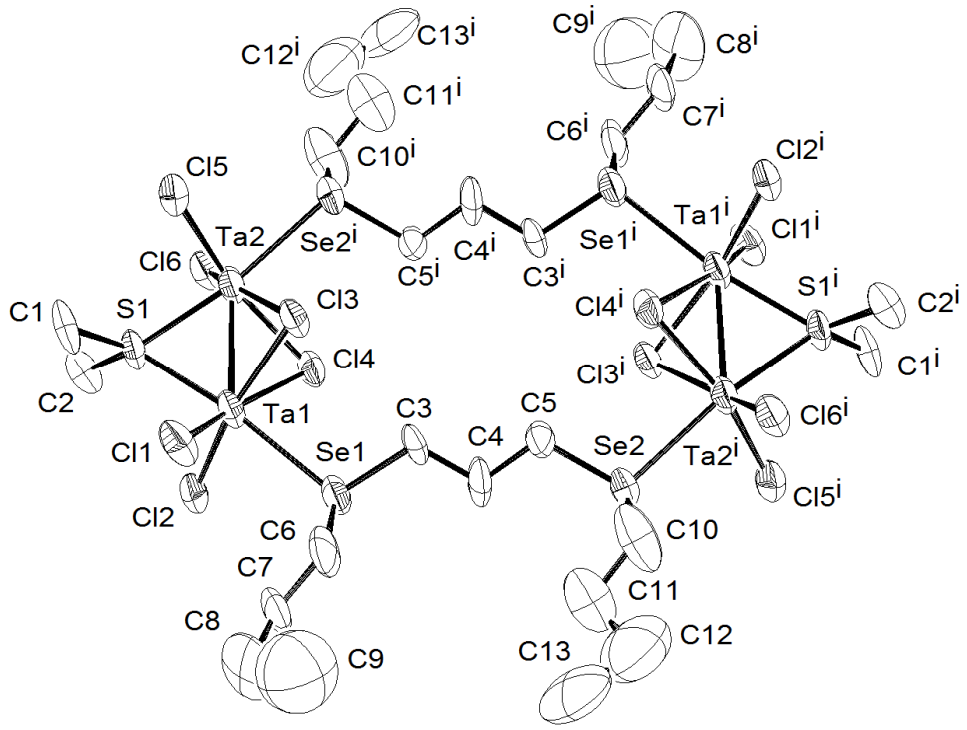

Figure 6. The structure of $[\{Ta_2Cl_4(\mu\text{-}Cl)_2(\mu\text{-}Me_2S)\}_2(\mu\text{-}^nBuSe(CH_2)_3Se^nBu)_2]$ showing the atom numbering scheme and with ellipsoids drawn at the 50% probability level. There is disorder in the Bu groups. Hydrogen atoms are omitted for clarity. Selected bond lengths (Å) and angles (°): Ta1–Cl2 = 2.377(6), Ta1–Cl1 = 2.385(8), Ta1–S1 = 2.389(6), Ta1–Cl4 = 2.486(7), Ta1–Cl3 = 2.517(6), Ta1–Ta2 = 2.6802(16), Ta1–Se1 = 2.740(3), Ta2–Cl6 = 2.366(7), Ta2–Cl5 = 2.382(7), Ta2–S1 = 2.392(7), Ta2–Cl3 = 2.501(6), Ta2–Cl4 = 2.522(7), Ta2–Se2 = 2.731(3), Ta2–Cl3–Ta1 = 64.56(15), Ta1–Cl4–Ta2 = 64.71(18), Ta1–S1–Ta2 = 68.19(18).

A few weakly diffracting crystals of a niobium analogue, $[\{Nb_2Cl_4(\mu\text{-}Cl)_2(\mu\text{-}Me_2S)\}_2(\mu\text{-}MeSeCH_2CH_2CH_2SeMe)_2]$, were obtained similarly, and the structural unit is very similar to that of the tantalum complex. The weak data precludes detailed comparisons of bond lengths or angles, but serves to identify the complex (see Supplementary Data). A literature precedent for the formation of the "dimer of dimers" structure is $[\{Ta_2Cl_4(\mu\text{-}Cl)_2(\mu\text{-}SC_4H_8)\}_2(\mu\text{-}Ph_2PCH_2CH_2PPh_2)_2]$, where the tantalum is coordinated to a bridging thiophene and the dimers are linked by diphosphine bridges [29].

The xylyl-linked diselenoether, $o\text{-}C_6H_4(CH_2SeMe)_2$, forms chelate complexes with late d-block metals and low valent metal carbonyls [30], but the C–Se links are very readily cleaved by strongly Lewis acidic metal centres [31] (contrasting with diselena-alkanes), and it was not surprising that reaction of $[Ta_2Cl_4(Me_2S)_2(\mu\text{-}Cl)_2(\mu\text{-}Me_2S)]$ with $o\text{-}C_6H_4(CH_2SeMe)_2$ gave a mixture of products. These included the orange-brown $[Ta_2Cl_4\{o\text{-}C_6H_4(CH_2SeMe)_2\}_2(\mu\text{-}Se)_2]$ obtained as a minor product, and identified by

its X-ray crystal structure (Figure. 7). This shows a Ta_2^{8+} with selenide bridges and the long Ta1–Ta1^{i} = 2.8999(12) Å, as expected for a single bond. The Ta–Se distances to the bridging selenide are ~ 0.3 Å shorter than the Ta–$Se_{(xylyl)}$ involving the neutral chelates which adopt the *DL* configuration.

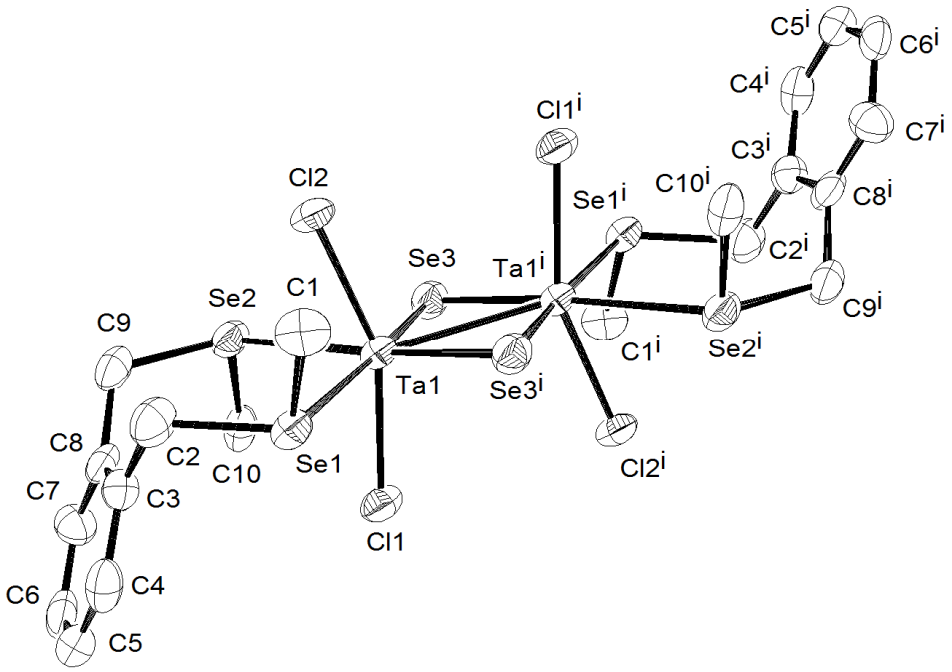

Figure 7. The structure of [Ta_2Cl_4{*o*-$C_6H_4(CH_2SeMe)_2$}$_2$(μ-Se)$_2$] showing the atom numbering scheme and with ellipsoids drawn at the 50% probability level. Hydrogen atoms are omitted for clarity. Selected bond lengths (Å) and angles (°): Ta1–Cl1 = 2.351(3), Ta1–Cl2 = 2.375(3), Ta1–Se3 = 2.4844(17), Ta1^{i}–Se3 = 2.4885(15), Ta1–Se1 = 2.7784(17), Ta1–Se2 = 2.7834(15), Ta1–Ta1^{i} = 2.8999(12), Ta1–Se–Ta1^{i} = 71.34(4).

3.4 Prospects as CVD Reagents

Attempts to deposit ME_2 films by low-pressure CVD used the equipment described elsewhere [13] which was successfully employed to deposit $NbSe_2$ from [$NbCl_5$($^{n}Bu_2Se$)]. At temperatures of 650–700°C and a pressure of 0.5 mmHg, the examination of various of the complexes of types [$M_2Cl_4(R_2S)_2$(*μ*-Cl)$_2$(*μ*-R_2S)] and [$M_2Cl_4(RECH_2CH_2ER)_2$(μ-Cl)$_2$] (E = S or Se) showed that they decomposed without evaporation, probably a consequence of their high molecular weights. As indicated in the Introduction, AACVD is a possible alternative route, requiring reagents soluble in an appropriate solvent such as hexane or toluene, with the solution introduced into the furnace as an aerosol. Unfortunately, the complexes like [$Ta_2Cl_4(Me_2S)_4$(μ-S)$_2$], which already contain some M-sulfide bonds and hence look promising precursors, are very poorly soluble in suitable solvents, and although we characterised a Se analogue, [Ta_2Cl_4{*o*-$C_6H_4(CH_2SeMe)_2$}$_2$(μ-Se)$_2$], this has not been

obtained in sufficient quantity to be useful as a CVD reagent. Other potential selenium reagents such as $[M_2Cl_4\{RSe(CH_2)_nSeR\}_2(\mu\text{-}Cl)_2]$ were relatively poorly soluble and unstable in solution. Although modifications using different R-groups could be investigated to improve solubility, the solution decomposition seems to rule out these Nb and Ta dimer complexes as viable CVD reagents.

3.5 Conclusions

A series of new dinuclear Nb(III) and Ta(III) thioether complexes, as well as the first fully authenticated examples with neutral selenoether coordination have been prepared, with confacial bi-octahedral or edge-bridged bi-octahedral geometries. Structural characterisation confirms the occurrence of M=M units. In some instances, either through prolonged reaction with *o*-$C_6H_4(CH_2SeMe)_2$, or, through addition of Me_2S_2, selenide or sulfide bridged Ta(IV) species were isolated in low yield. These complexes are not sufficiently volatile or stable in solution to be suitable as single source precursors for either low pressure or aerosol assisted CVD of niobium or tantalum chalcogenide films.

Acknowledgements

We thank the University of Southampton for support.

Appendix A. Supplementary data

The X-ray crystal structures of $[\{Nb_2Cl_4(\mu\text{-}Cl)_2(\mu\text{-}Me_2S)\}_2(\mu\text{-}MeSeCH_2CH_2CH_2SeMe)_2]$ and $[Ta_2Cl_4S_2(Me_2S)_4]$.

References

1. T. Waters, A. G. Wedd, M. Ziolek, I. Nowak, in T. J. Meyer, J. A. McCleverty (Eds) Comprehensive Coordination Chemistry II, Elsevier, Oxford (2004) vol. 4, Chapter 5.
2. J. Liu, X.-W. Liu, Adv. Mater. 24 (2012) 4097–4111.
3. K. Lee, R. Gatensby, N. McEvoy, T. Hallam, G. S. Duesberg, Adv. Mater. 25 (2013) 6699–6702.

4. M. Chhowalla, H. S. Shin, G. Eda, L.-J. Li, K. P. Loh, H. Zhang, Nat. Chem. 5 (2013) 263–275.

5. Q. Xiang, J. Yu, M. Jaroniec, J. Am. Chem. Soc. 134 (2012) 6575–6578.

6. H. Zeng, J. Dai, W. Yao, D. Xiao, X. Cui, Nanotechnol. 7 (2012) 490–493.

7. Y. Ma, Y. Dsi, M. Guo, C. Niu, Y. Zhu, B. Huang, ACS Nano 6 (2012) 1695–1701.

8. K. Xu, P. Chen, X. Li, C. Wu, Y. Guo, J. Zhao, X. Wu, Y. Xie, Angew. Chem., Int. Ed. 52 (2013) 10477–10481.

9. A. C. Jones and M. L. Hitchman, in Chemical Vapour Deposition: Precursors, Processes and Applications, Royal Society of Chemistry (2009).

10. N. D. Boscher, C. J. Carmalt. I. P. Parkin, Eur. J. Inorg. Chem. (2006) 1255–1259; E. Peters, C. J. Carmalt, I. P. Parkin, D. A. Tocher, Eur. J. Inorg. Chem. (2005) 4179-4185; C. J. Carmalt, E. S. Peters, I. P. Parkin, T. D. Manning, A. L. Hector, Eur. J. Inorg. Chem. (2004) 4470–4476.

11. P. J. McKarns, T. S. Lewkebandara, G. P. A. Yap, L. M. Liable-Sands, A. L. Rheingold and C. H. Winter, Inorg. Chem. 37 (1998) 418–424; S. D. Reid, A. L. Hector, W. Levason, G. Reid, B. J. Waller, M. Webster, Dalton Trans. (2007) 4769–4777; S. L. Benjamin, C. H. de Groot, C. Gurnani, A. L. Hector, R. Huang, K. Ignatyev, W. Levason, S. J. Pearce, F. Thomas, G. Reid, Chem. Mater. 25 (2013) 4719–4724.

12. A. L. Hector, M. Jura, W. Levason, S. D. Reid, G. Reid, New J. Chem. 33 (2009) 641–645; A. L. Hector, W. Levason, G. Reid, S. D. Reid, M. Webster, Chem. Mater. 20 (2008) 5100–5116.

13. S. L. Benjamin, Y.-P. Chang, C. Gurnani, A. L. Hector, M. Huggon, W. Levason, G. Reid, Dalton Trans. 43 (2014) 16640–16648.

14. A. D. Allen, S. Naito, Can. J. Chem. 54 (1976) 2948–2952.

15. F. A. Cotton, R. C. Najjar, Inorg. Chem. 20 (1981) 2716–2719.

16. M. Matsuura, T. Fujihara, M. Kakeya, T. Sugaya, A. Nagasawa, J. Organomet. Chem. 745-746 (2013) 288–298.

17. M. Kakeya, T. Fujihara, A. Nagasawa, Acta Crystallogr. E62 (2006) m553–m554.

18. J. A. Canich, F. A. Cotton, Inorg. Chem. 26 (1987) 3473–3478.

19. M. E. Clay, T. M. Brown, Inorg. Chim. Acta 72 (1983) 75–80.

20. G. C. Campbell, J. A. Cranich, F. A. Cotton, S. A. Duraj, J. F. Haw, Inorg. Chem. 25 (1986) 287–290.

21. E. Babaian-Kibala, F. A. Cotton, P. A. Kibala, Inorg. Chem. 29 (1990) 4002–4005.

22. F. R. Hartley, S. G. Murray, W. Levason, H. E. Soutter, C. A. McAuliffe, Inorg. Chim. Acta 35 (1979) 265–277; D. J. Gulliver, E. G. Hope, W. Levason, S. G. Murray, D. M. Potter, G. L. Marshall, J. Chem. Soc. Perkin Trans. II (1984) 429–434.

23. M. Tsunoda, L. G. Hubert-Pfalzgraf, Inorg. Synth. 21 (1982) 16–18.

24. G. M. Sheldrick, Acta Crystallogr. A64 (2008) 112–122.

25. F. A. Cotton and R. A. Walton, Multiple Bonds between Metal Atoms, Oxford, 1993, 2nd ed Chapter 9; F. A. Cotton, X. Feng, P. Gutlich, T. Kohlhaas, J. Lu, M. Shang, Inorg. Chem. 33 (1994) 3055–3063.

26. E. W. Abel, S. K. Bhargava, K. G. Orrell, Progr. Inorg. Chem. 32 (1984) 1–118.

27. N. P. Lutra, J. D. Odom, in The chemistry of organic selenium and tellurium compounds, S. Patai, Z. Rappoport (Eds), Wiley NY. 1 (1986) Chapter 6.

28. R. Hart, W. Levason, B. Patel, G. Reid, J. Chem. Soc., Dalton Trans. (2002) 3153–3159.

29. P. F. Gilletti, V. G. Young, T. M. Brown, Inorg. Chem. 28 (1989) 4034-4036.

30. W. Levason, M. Nirwan, R. Ratnani, G. Reid, N. Tsoureas, M. Webster, Dalton Trans. (2007) 439–448; W. Levason, L. P. Ollivere, G. Reid, N. Tsoureas, M. Webster. J. Organometal. Chem. 694 (2009) 2299-2308

31. C. Gurnani, W. Levason, R. Ratnani, G. Reid, M. Webster, Dalton Trans. (2008) 6274–6282; C. Gurnani, M. Jura, W. Levason, R. Ratnani, G. Reid, M. Webster, Dalton Trans. (2009), 1611–1619.

Table 1 Crystal data and structure refinement details[a]

Compound	$[Nb_2Cl_6(^nBu_2S)_3]$	$[Ta_2Cl_6(^nBu_2S)_3]$	$[Ta_2Cl_8(Me_2S)_2]$	$[Ta_2Cl_6(Me_2S)_3]$
Formula	$C_{24}H_{54}Cl_6Nb_2S_3$	$C_{24}H_{54}Cl_6S_3Ta_2$	$C_4H_{12}Cl_8S_2Ta_2$	$C_6H_{18}Cl_6S_3Ta_2$
Formula weight	837.37	1013.45	769.76	760.98
Crystal system	Monoclinic	Monoclinic	Monoclinic	Orthorhombic
Space group (no)	C2/c (15)	C2/c (15)	$P2_1/n$ (14)	Pbcn (60)
a/ Å	27.1516(10)	27.3170(10)	6.500(6)	13.003(5)
b/ Å	20.1757(8)	20.3709(10)	10.148(9)	13.574(5)
c/ Å	20.8202(15)	20.9320(10)	13.252(16)	10.543(4)
α/deg	90	90	90.866(9)	90
β/ deg	102.842(7)	103.0350(10)	94.219(7)	90
γ/ deg	90	90	90	90
U/ $Å^3$	11120.1(10)	11347.9(9)	871.8(15)	1861.0(11)
Z	12	12	2	4
μ(Mo-Kα)/mm^{-1}	1.234	6.384	13.981	12.928
F(000)	5160	5928	700	1400
Total number reflns	36917	48314	4935	4173
R_{int}	0.072	0.068	0.031	0.128
Unique reflns	12709	11094	1977	2118
No. of params, restraints	500, 55	501, 34	75, 0	78, 0
R_1[b] $[I_o>2\sigma(I_o)]$	0.067	0.0552	0.0230,	0.072
R_1 (all data)	0.110	0.060	0.026	0.176
wR_2[b] $[I_o>2\sigma(I_o)]$	0.171	0.140	0.056	0.133
wR_2 (all data)	0.1902	0.1449	0.058	0.169

a Common items: temperature = 100 K; wavelength (Mo-K_α) = 0.71073 Å; θ(max) = 27.5°. b $R_1 = \Sigma \big| |F_o| - |F_c| \big| / \Sigma |F_o|$; $wR_2 = [\Sigma w(F_o^2 - F_c^2)^2 / \Sigma wF_o^4]^{1/2}$

Table 1 continued

Compound	$[Ta_2Cl_4Se_2(o\text{-}C_6H_4(CH_2SeMe)_2)]$	$[\{Ta_2Cl_6(SMe_2)_2(^nBuSeCH_2CH_2CH_2Se^nBu)\}_2]$
Formula	$C_{20}H_{28}Cl_4Se_6Ta_2$	$C_{26}H_{60}Cl_{12}S_2Se_4Ta_4$
Formula weight	1245.88	1901.90
Crystal system	Monoclinic	Triclinic
Space group	$P2_1/c$ (14)	P-1 (2)
a/ Å	9.2046(8)	8.0202(9)
b/ Å	10.4069(8)	11.4792(14)
c/ Å	15.6689(14)	14.7514(19)
α/deg	90	90.866(9)
β/ deg	99.410(7)	91.623(6)
γ/ deg	90	110.333(5)
U/ $Å^3$	1480.7(2)	1272.5(3)
Z	2	1
μ(Mo-Kα)/mm^{-1}	15.130	12.163
F(000)	1132	880
Total number reflns	7205	9647
R_{int}	0.066	0.108
Unique reflns	3382	4975
No. of params, restraints	145, 0	212, 34
$R_1{}^b$ $[I_o>2\sigma(I_o)]$	0.063	0.091
R_1 (all data)	0.102	0.179
$wR_2{}^b$ $[I_o>2\sigma(I_o)]$	0.124	0.193
wR_2 (all data)	0.146	0.245

Supplementary Information

Dinuclear niobium(III), tantalum(III) and tantalum(IV) complexes with thioether and selenoether ligands

Sophie L. Benjamin, Yao-Pang Chang, Michelle Huggon, William Levason and Gillian Reid

$[\{Nb_2Cl_4(\mu\text{-}Cl)_2(\mu\text{-}Me_2S)\}_2(\mu\text{-}MeSeCH_2CH_2CH_2SeMe)_2]$

A pure sample could not be obtained on a preparative scale, however, a few small crystals were obtained by layering solutions $[Nb_2Cl_4(Me_2S)_2(\mu\text{-}Cl)_2(\mu\text{-}Me_2S)]$ in toluene and $MeSeCH_2CH_2CH_2SeMe$ in n-hexane. After one week, a few purple crystals were observed. These small, weakly diffracting crystals were analysed by X-ray diffraction: monoclinic, space group $P2_1/c$ (no. 14), a = 12.586(6), b = 12.945(6), c = 11.919(5) Å, β = 92.24(1)°, V = 1940.62 Å^3, Z = 4, R_1, wR_2 ($I > 2\sigma(I)$) = 0.134, 0.346. The rather poor data quality precludes detailed comparisons, but serves to identify a second example of the "dimer of dimers" type in this work.

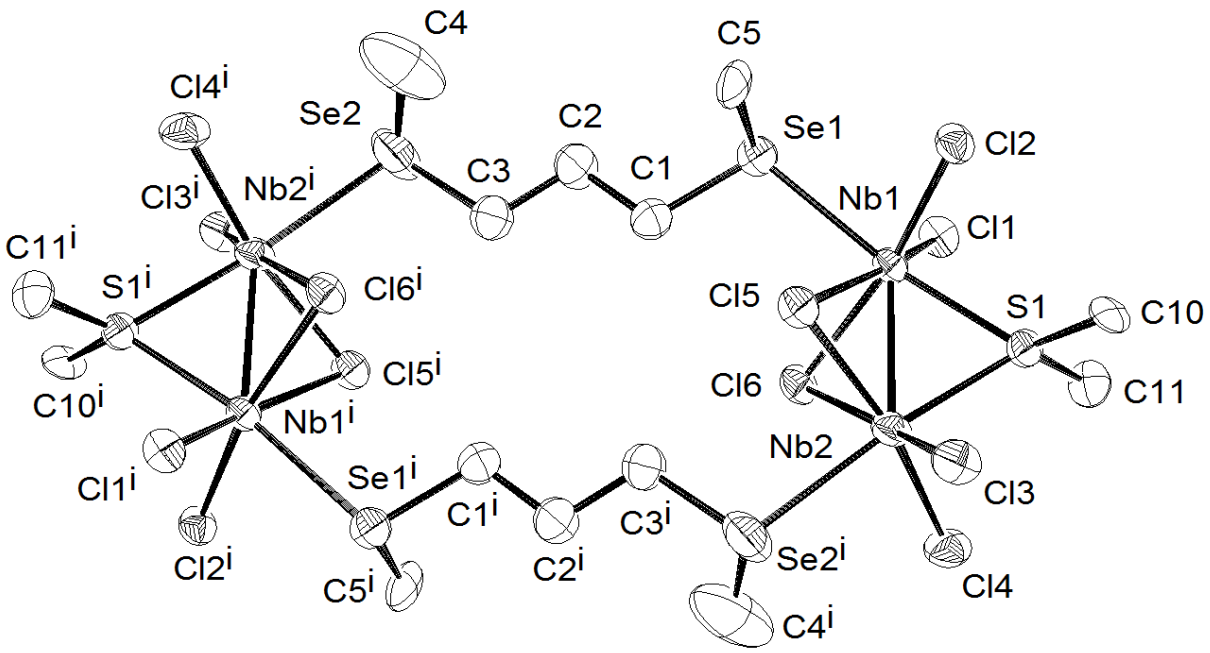

Figure S1. The structure of $[\{Nb_2Cl_4(\mu\text{-}Cl)_2(\mu\text{-}Me_2S)\}_2(\mu\text{-}MeSeCH_2CH_2CH_2SeMe)_2]$ with the atom numbering scheme.

Table S1 Crystal data and structure refinement details

Compound	$[Ta_2Cl_4S_2(Me_2S)_4]$
Formula	$C_8H_{24}Cl_4S_6Ta_2$
Formula weight	816.33
Crystal system	Monoclinic
Space group	$P2_1/n$ (14)
a/ Å	10.2420(8)
b/ Å	10.9439(9)
c/ Å	10.3916(8)
α/deg	90
β/ deg	96.813(5)
γ/ deg	90
U/ $Å^3$	1156.54(16)
Z	2
μ(Mo-Kα)/mm^{-1}	10.447
F(000)	764
Total number reflns	7108
R_{int}	0.039
Unique reflns	2272
No. of params, restraints	95, 0
R_1[b] [$I_o>2\sigma(I_o)$]	0.020
R_1 (all data)	0.025
wR_2[b] [$I_o>2\sigma(I_o)$]	0.039
wR_2 (all data)	0.040

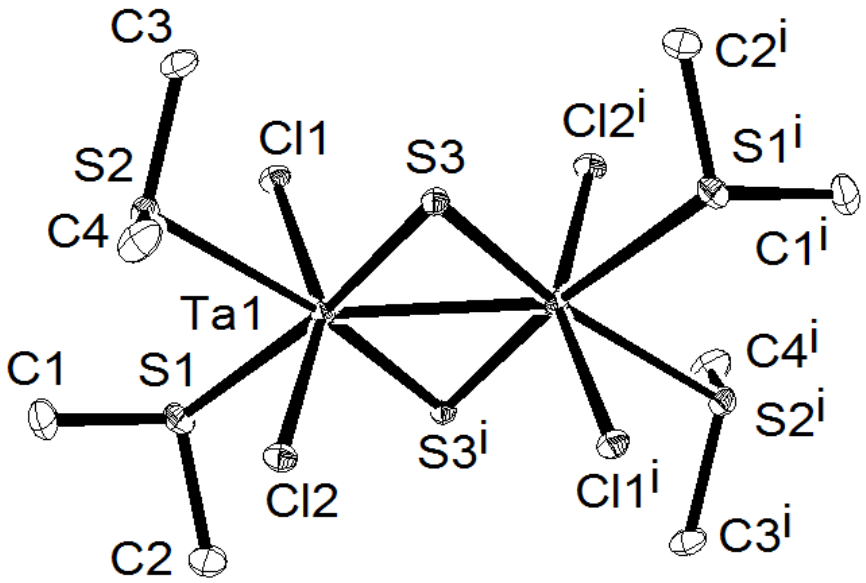

Figure S2 Structure of $[Ta_2Cl_4(Me_2S)_4(\mu\text{-}S)_2]$ showing the atom numbering scheme. Ellipsoids are drawn at the 50% level. Hydrogen atoms are omitted for clarity. Selected bond lengths (Å) and angles (°): Ta1–Cl1 = 2.3779(8), Ta1–Cl2 = 2.3657(8), Ta1–S1 = 2.6842(9), Ta1–S2 = 2.7179(9), Ta1–S3 = 2.3513(9), Ta1–$S3^i$ = 2.3574(9), Ta1–$Ta1^i$ = 2.8368(3), Ta1–S3–$Ta1^i$ = 74.09(3).

Contents Page

Dinuclear niobium(III), tantalum(III) and tantalum(IV) complexes with thioether and selenoether ligands

Sophie L. Benjamin, Yao-Pang Chang, Michelle Huggon, William Levason and Gillian Reid

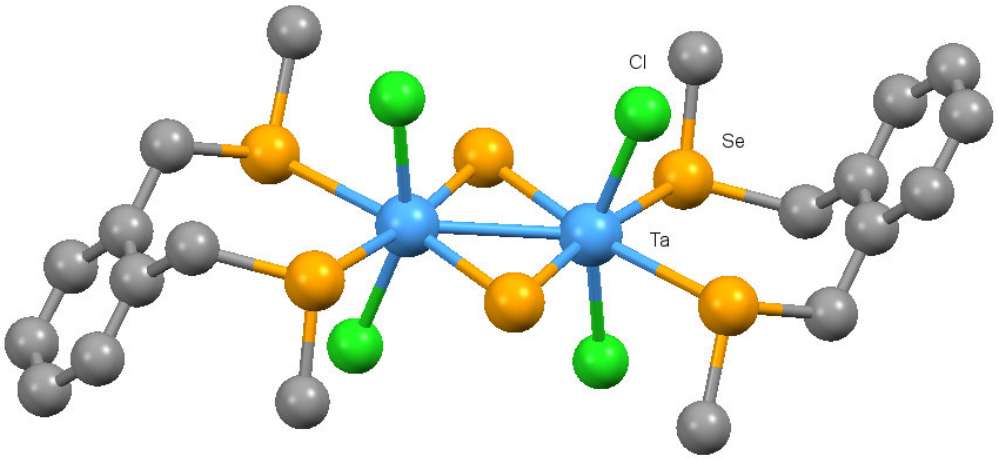

Contents Page

Dinuclear niobium(III), tantalum(III) and tantalum(IV) complexes with thioether and selenoether ligands

Sophie L. Benjamin, Yao-Pang Chang, Michelle Huggon, William Levason and Gillian Reid

A series of dinuclear Nb(III), Ta(III) and Ta(IV) complexes with neutral sulfur and selenium ligands are described, together with spectroscopic and structural characterisation.